

## 10. HOPPER DESIGN

People have stored powdered materials for thousands of years, at least as far back as man has harvested and stored crops. Prior to the 1960s storage bins were designed largely by guessing. This was all changed by the research of Andrew W. Jenike in the 1960s. His work identified the criteria that affect material flow in storage vessels. Jenike developed the theory and methods to apply the theory, including the equations and measurement of the necessary material properties. His primary works are published in "Gravity Flow of Bulk Solids", Bulletin 108, University of Utah Engineering Experiment Station, October 1961, and Bulletin 123, November 1964.\*

Hoppers are used in industry for protection and storage of powdered materials. Hoppers must be designed such that they are easy to load. More importantly, hoppers must be designed such that they are easy to unload.

The way the hopper is designed affects the rate of flow of the powder out of the hopper, *if it flows at all*. Also, the way the hopper is designed affects how much of the stored material can discharge and whether there mixing of solid sizes or dead space that reduces the effective holding capacity of the hopper. These issues and others discussed here are important to consider when designing storage hoppers.

### 10.1 Flow Modes

There are two primary and distinct types of flow of solids in hoppers, *mass flow* and *funnel flow*. There is also a special case that is a combination of these two flows called *expanded flow*. These flows get their names from the way in which solids move in the hoppers. The characteristics and differences between the flows are depicted in Figure 10-1.

The primary difference between mass and funnel flow is that in mass flow all of the material in the bin is in motion, though not necessarily all with the same velocity. In funnel flow only a core of material in the center above the hopper outlet is in motion while material next to the walls is stationary (stagnant).

Hoppers come in a variety of shapes and designs, not just conical. Figure 10-2 shows some of the more common designs found for mass flow hoppers. Also, a variety of designs are possible for funnel flow hoppers, shown in Figure 10-3.

\* Other references that give a good summary on this topic include:

1. J. Bridgwater and A.M. Scott, "Flow of Solids in Bunkers," in Handbook of Fluids in Motion, N.P. Cheremisinoff and R. Gupta eds., Butterworth, Ann Arbor, chapter 31, 807-846, 1983.
2. R. Holdich, Fundamentals of Particle Technology, Midland, Loughborough, UK, 2002.
3. M. Rhodes, Principles of Powder Technology, Wiley, New York, 1990.

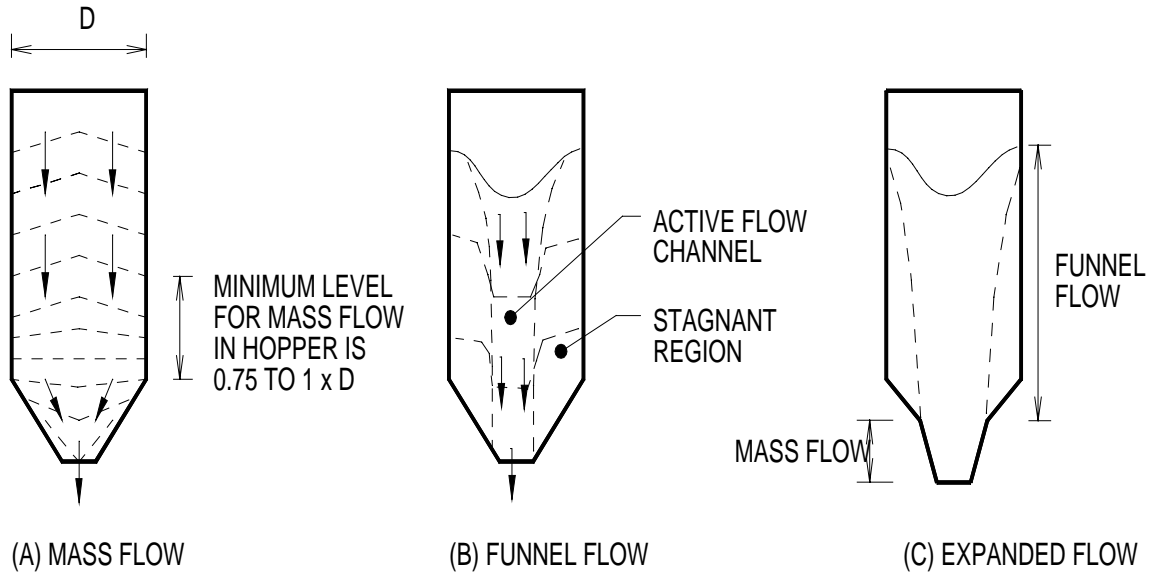


Figure 10-1. In mass flow (A) all material moves in the bin including near the walls. In funnel flow (B) the material moves in a central core with stagnant material near the walls. Expanded flow (C) is a combination of mass flow in the hopper exit and funnel flow in the bin above the hopper (normally used in retrofit situations).

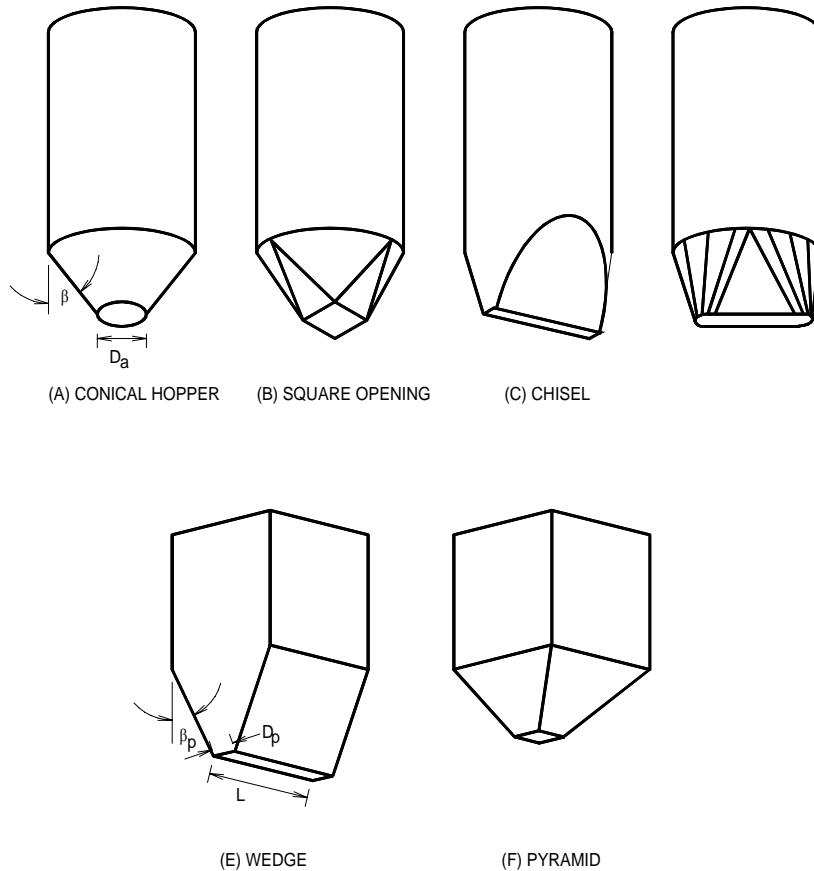


Figure 10-2. Common designs for mass flow hoppers.

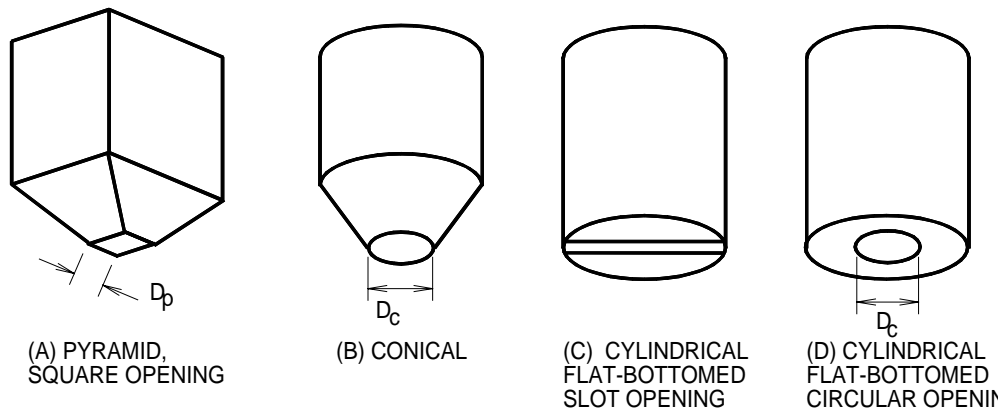


Figure 10-3. Common designs for funnel flow hoppers.

## 10.2 Hopper Design Problems

Hopper design problems are normally one of two types; either the material does not discharge adequately from the opening in the hopper or the material segregates during the flow. The problems that we would like to solve or avoid are

- **RATHOLING/PIPING.** Ratholing or piping occurs when the core of the hopper discharges (as in funnel flow) but the stagnant sides are stable enough to remain in place without flowing, leaving a hole down through the center of the solids stored in the bin (See Figure 10-4a).
- **FLOW IS TOO SLOW.** The material does not exit from the hopper fast enough to feed follow on processes.
- **NO FLOW DUE TO ARCHING OR DOMING.** The material is cohesive enough that the particles form arch bridges or domes that hold overburden material in place and stop the flow completely (Figure 10-4b).
- **FLUSHING.** Flushing occurs when the material is not cohesive enough to form a stable dome, but strong enough that the material discharge rate slows down while air tries to penetrate into the packed material to loosen up some of the material. The resulting effect is a sluggish flow of solids as the air penetrates in a short distance freeing a layer of material and the process starts over with the air penetrating into the freshly exposed surface of material (Figure 10-4c).
- **INCOMPLETE EMPTYING.** Dead spaces in the bin can prevent a bin from complete discharge of the material.

- **SEGREGATION.** Different size and density particles tend to segregate due to vibrations and a percolation action of the smaller particles moving through the void space between the larger particles.

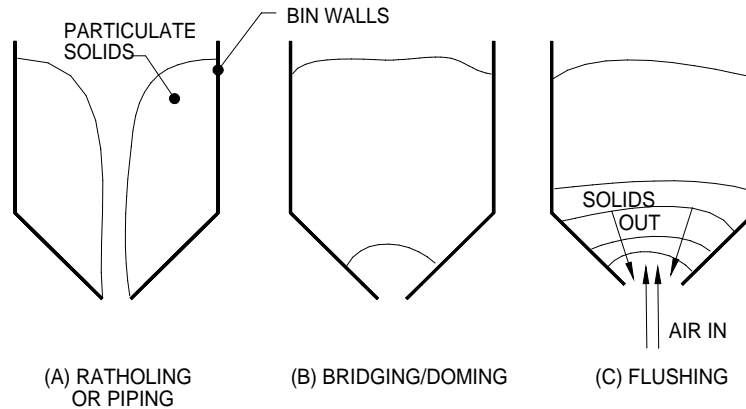


Figure 10-4. Common problems in bin/hopper design.

- **TIME CONSOLIDATION.** For many materials, if allowed to sit in a hopper over a long period of time the particles tend to rearrange themselves so that they become more tightly packed together. This effect is referred to as Dense Packing by Foust in the bed porosity in Figure 4-5. The consolidated materials are more difficult to flow and tend to bridge or rat hole.
- **CAKING.** Another important effect is called caking. Caking refers to the physiochemical bonding between particles what occurs due to changes in humidity. Moisture in the air can react with or dissolve some solid materials such as cement and salt. When the air humidity changes the dissolved solids re-solidify and can cause particles to grow together. A good description of this effect is given by Griffith (E.J. Griffith, *Cake Formation in Particulate Systems*, VCH Publishers, NY, 1991).

### 10.3 Predicting Mass Flow

Many of the problems associated with bin and hopper design can be avoided by designing the hopper to operate in mass flow mode. The required cone angle from the vertical axis for mass flow to occur ranges from 40° to 0°.

Mass flow is not necessary in all cases. In some situations a mass flow hopper design is not practical due to the head room required. Table 10-1 summarizes the key advantages and disadvantages of both mass flow and funnel flow hoppers. In most applications if you have a choice you want mass flow. But in the extreme cases or in cases in which mass flow is not really necessary then you may opt for the shorter funnel flow hopper design.

Table 10-1. Advantages and Disadvantages of Mass and Funnel Flow Hoppers

	MASS FLOW	FUNNEL FLOW
ADVANTAGES	<ul style="list-style-type: none"> <li>• Flow is more consistent</li> <li>• Reduced radial segregation</li> <li>• Stresses on walls are more predictable</li> <li>• Effective use of full bin capacity</li> <li>• First-in = First-out</li> </ul>	<ul style="list-style-type: none"> <li>• Low head room required</li> </ul>
DISADVANTAGES	<ul style="list-style-type: none"> <li>• More wear of wall surfaces</li> <li>• Higher stresses on the walls</li> <li>• More head room required</li> </ul>	<ul style="list-style-type: none"> <li>• Rat holing</li> <li>• Segregation</li> <li>• First-in = Last-out</li> <li>• Time consolidation effects can be severe</li> <li>• Poor distribution of stresses on walls may cause silo collapse</li> <li>• Flooding</li> <li>• Reduction of effective storage capacity.</li> </ul>

### 10.3.1 BINDING MECHANISMS

There are a number of mechanisms that cause solid materials to bind together and thus make flow difficult if not impossible. Some of these have been mentioned above.

Binding mechanisms include:

1. Solids Bridge (*ie.* Caking)
  - Mineral Bridges
  - Chemical reactions
  - Partial melting
  - Binder hardening
  - Crystallization of dissolved substances
2. Adhesion and Cohesion
  - There are a number of effects that are lumped together and are termed adhesion and cohesion. These include mechanically deformable particles that can plastically deform and bind to each other or with bin walls. Usually, very small particles display adhesion properties.
3. Interfacial forces.

- Interfacial forces include liquid bridges and capillary forces between particles. These effects are due the contact surfaces between three phases (solid, liquid and gas) and interfacial tensions.
4. Attractive forces.
    - Attractive forces include intermolecular forces such as van der Waal's force, as well as longer range electrostatic and magnetic forces. There are also short range repulsive forces, but if the particles are in close enough contact the attractive forces are stronger.
  5. Interlocking forces.
    - Interlocking forces are due to the geometric entanglement that occurs with fibrous materials, analogous to what happens when you store coat hangers in a box - they become entangled.

Many earlier bin designs were based upon the angle of repose (see Chapter 4). However, the angle of repose alone is not sufficient to account for all of the mechanisms affecting hopper performance. The angle of repose is only useful in determining the contour of a pile, and its popularity among engineers is not due to its usefulness but due to the ease with which it can be measured.

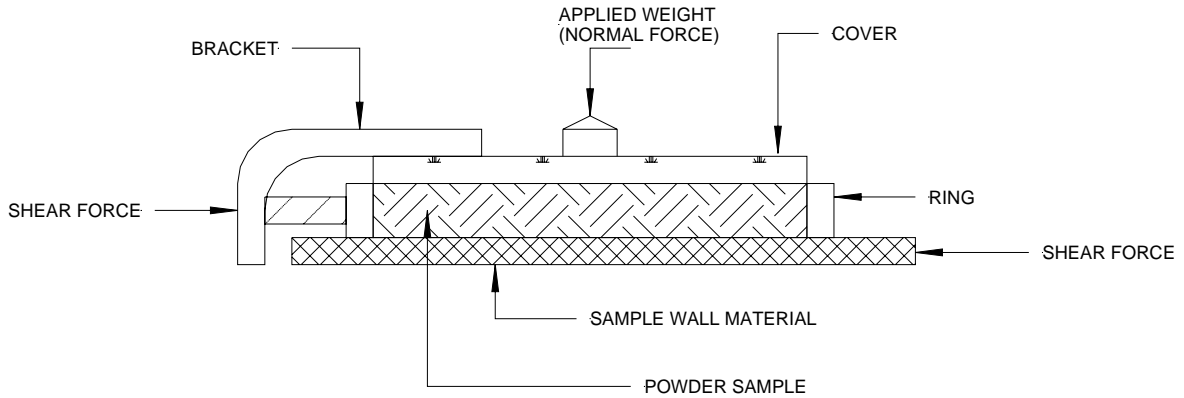
### 10.3.2 TESTING REQUIREMENTS

To design storage hoppers, the following material properties are needed:

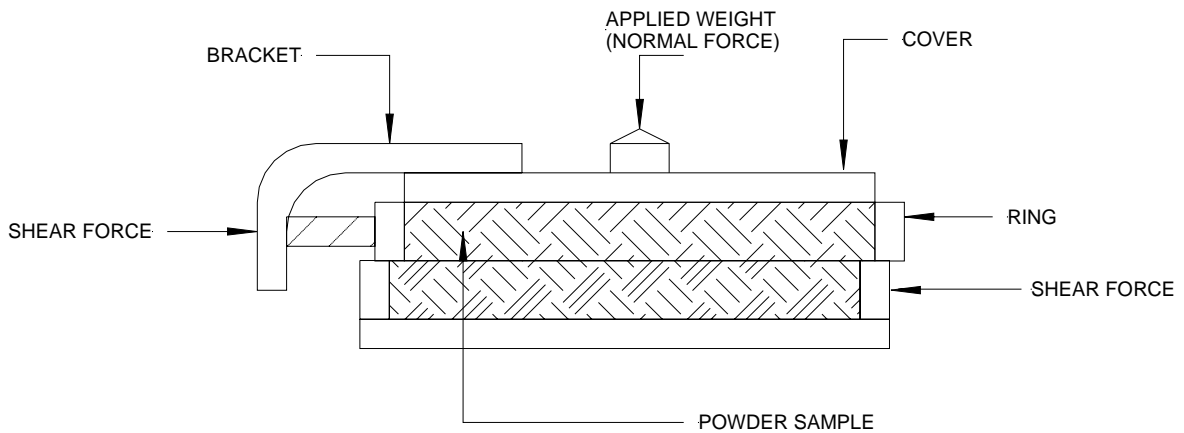
- Internal friction coefficient
- Wall friction coefficient
- Permeability
- Compressibility

Other factors that should be considered include temperature and moisture content along with phase diagrams if caking may be a problem.

One of the more common test apparatus is the Jenike Shear Tester. The Jenike Shear Tester has similarity to the Triaxial shear tester mentioned in Chapter 4. The powder sample is placed in a sample holder. The movement of the sample holder causes shear between a powder sample and a sample of the hopper wall as in Figure 10-5(a) to determine the wall friction coefficient. Or, the movement causes a shear internally in the powder sample as in Figure 10-5(b) to determine the internal coefficient of friction.



(a) Wall Friction Test. The powder sample is in contact with a wall sample. Shearing occurs between the powder and wall samples.



(b) Internal Friction Test. The powder sample is sheared within itself.

Figure 10-5. Internal and wall friction tests with the Janike Shear Tester.

The friction tests are simple application of physics to determine the friction coefficients as discussed in Chapter 4 where the shearing force  $F$  is related to the normal force  $N$  by the coefficient of friction  $\mu$  in the equation

$$F = \mu N \quad (10-1)$$

As commonly practiced, the coefficient of friction is expressed as the “angle” of wall friction given by  $\phi$  as

$$\phi = \arctan(\mu). \quad (10-2)$$

Other shear test devices are available commercially, such as the rotating disk test called Peschl Tester, developed by I.A.S.Z. Peschl of The Netherlands, which operates by placing a sample between two circular disks and rotating the disks about their center axis relative to one another. This has an advantage over the Jenike Shear tester because the

shearing can occur for longer periods of time, giving the particles opportunity to compact. However friction between the moving parts of the sample holder can cause doubt about the accuracy of the measured results and there are some doubts about the assumed zero stress at the center of the rotating disks.

Another test that has been around for many years is the annular shear cell. As with the rotating disk tester, the annular shear cell has infinite travel. The sample is placed in the annular space between two cylinders. A cover is placed on top of the sample to hold the powder in the annular space and to apply the desired normal force. The cover is rotated relative to the rest of the assembly, causing shearing of the sample. This device is good for elastic materials and for pastes. The measured results have not been fully tested for use in bin design and sealing powders can be a problem.

### 10.3.3 STRESSES IN HOPPERS AND SILOS

Consider the equilibrium of forces acting on a differential element,  $dz$ , in a straight sided cylindrical silo (Figure 10-6). In the stationary situation the surrounding fluid (air) pressure acts uniformly on all solid particles throughout the silo.

However, there are compressive normal stresses,  $P_v$ , acting on the cross sectional area,  $A$ , due to the overburden of material above the volume element. There are also shear stresses,  $\tau_R$ , of the solid phase acting on the silo walls. We list the various components contributing to the force in the z-direction:

Overburden normal stress acting downward on the surface at  $z$   $P_v A$

Normal stress acting upward on the surface at  $z + \Delta z$   $-(P_v + dP_v)A$

Shear stress acting on the silo walls acting upward  $-\tau_R \pi D dz$

Gravity force acting downward on the differential element  $\rho^o A dz g$

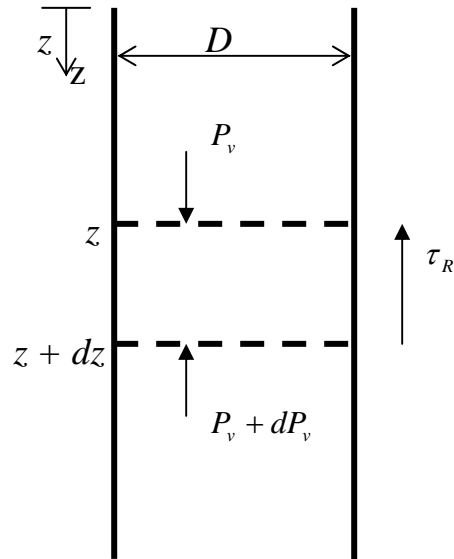


Figure 10-6. Differential force balance on a cylindrical storage bin.

At steady state (no accelerations, or neglecting inertial terms) the sum of the forces must equal zero. This gives the balance of forces as

$$A(P_v) - A(P_v + dP_v) - \tau_R \pi D dz + \rho^o A dz g = 0 \quad (10-3)$$

which reduces to

$$- A(dP_v) - \tau_R \pi D dz + \rho^o A dz g = 0 \quad (10-4)$$

From physics we relate the shear stress at the wall to the lateral normal stress acting in the radial direction at the wall,  $P_w$ , with the coefficient of friction,  $\mu$ ,

$$\tau_R = \mu P_w \quad (10-5)$$

Substitution of Eq.(10-5) into (10-4) gives

$$- A(dP_v) - \mu P_w \pi D dz + \rho^o A dz g = 0 \quad (10-6)$$

which has both  $P_w$  and  $P_v$  terms.

Janssen solved this equation (H.A. Janssen, Versuche über Getreidedruck in Silozellen, Verein Deutscher Ingenieure, Zeitschrift, **39**, August 1885, 1045-1049) by assuming that the vertical normal stress is proportional to the lateral normal stress (section 4.2.3), where

$$P_w = K P_v. \quad (10-7)$$

Substituting Eq. (10-7) into (10-6) and rearranging, where  $A = \frac{\pi D^2}{4}$ , we get

$$dP_v = -\frac{4\mu K}{D} \left( P_v - \frac{\rho^o g D}{4\mu K} \right) dz. \quad (10-8)$$

Equation (10-8) is integrated with the boundary condition that  $P_v = 0$  at  $z = 0$ , to obtain

$$P_v = \frac{\rho^o g D}{4\mu K g_c} \left( 1 - \exp\left(-\frac{4\mu K z}{D}\right) \right). \quad (10-9)$$

where the  $g_c$  is the gravity constant conversion factor to convert the result from units of mass to units of force. This latter expression is known as the Janssen Equation. When we plot the pressure in the silo as a function of depth from the free surface of the granular material at the top we get a plot as shown in Figure 10-7.

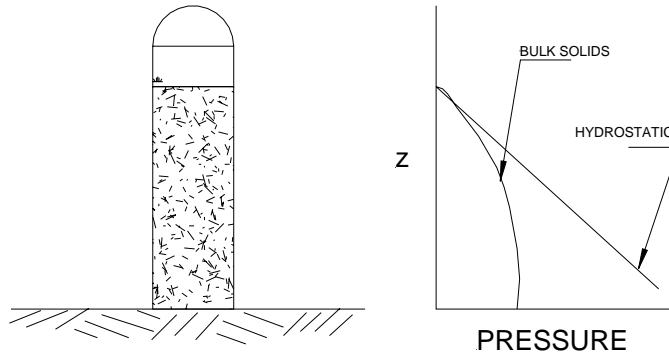


Figure 10-7. Vertical normal stress profile in a silo.

Note that in Figure 10-7 the asymptotic pressure for large depth is only a function of the silo diameter and not on depth. This is one reason why commercial silos are designed tall and narrow rather than short and squat.

At the bottom of the silo is the converging hopper section. Andrew Jenike (A.W. Jenike, Storage and Flow of Solids, Bulletin No. 123, Utah Engineering Experiment Station, University of Utah, Salt Lake City, Utah, 1964) postulated that the magnitude of stress in the converging section is proportional to the distance from the hopper apex (as well as a dependence on the angle). The stress is written as

$$\sigma = \sigma(r, \theta). \tag{10-10}$$

10) as indicated in Figure 10-8.

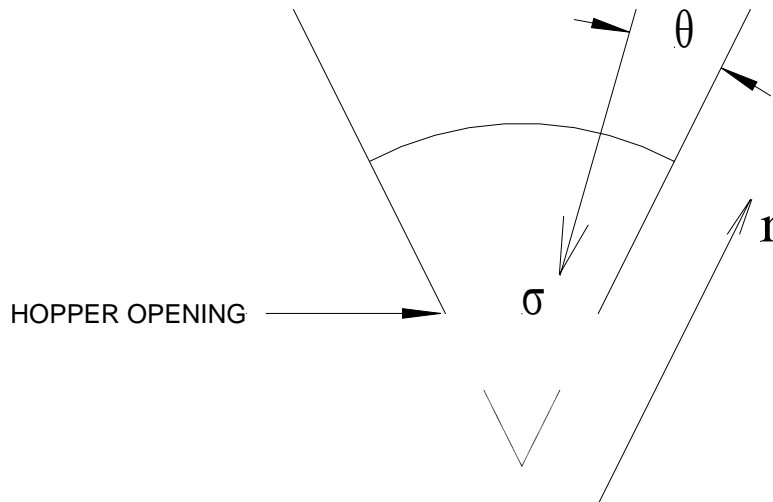


Figure 10-8. The stress,  $\sigma$ , in the hopper is a function of position  $(r, \theta)$ .

The rigorous calculations applying the radial stress field assumption are beyond the scope of this discussion. However, the results of those calculations shown in Figure 10-9 give us insight as to the conditions at the bottom of the silo at the hopper discharge. Figure 10-9 shows that there is essentially no stress at the hopper outlet. This is good because it allows dischargers such as screws and rotary valves to turn easily.

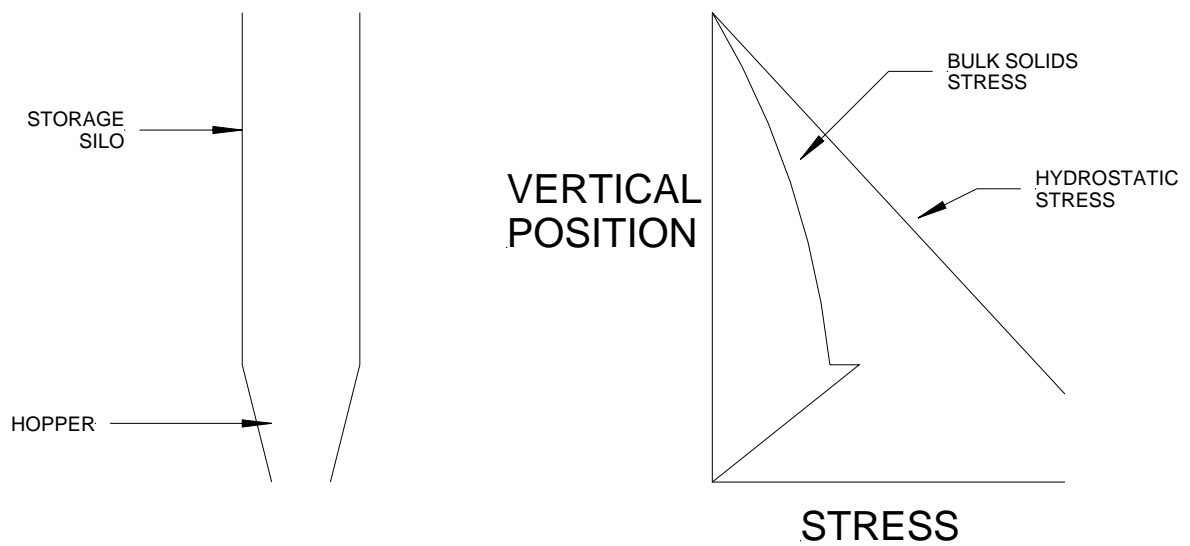


Figure 10-9. Hopper stress field including the stresses in the converging hopper discharge section.

**EXAMPLE 10-1. APPLICATION OF JANSSEN'S EQUATION**

A large welded steel silo 4 meters in diameter and 20 meters high is to be built. The silo has a central discharge on a flat bottom. Estimate the pressure on the wall at the bottom of the silo if the silo is filled with (a) plastic pellets, and (b) water. The plastic pellets have the following characteristics

$$\rho^o = 560 \text{ kg / m}^3$$

$$\phi = 20^\circ$$

*SOLUTION:*

(a) The Janssen Equation, Eq.(10-9), is for silos of circular cross section. Diameter and height are given in the problem statement. The coefficient of wall friction is obtained by inverting Eq.(10-2) as

$$\mu = \tan(20^\circ) = 0.364$$

$K$ , the Janssen Coefficient, is assumed to be 0.4. The Janssen coefficient can vary with material as indicated in Figure 4-4, but it is not often measured. Substituting these quantities into Eq.(10-9) we get the vertical stress at the bottom of the silo:

$$\begin{aligned} P_v &= \frac{\rho^o g D}{4\mu K g_c} \left( 1 - \exp\left(-\frac{4z\mu K}{D}\right) \right) \\ &= \frac{(560 \text{ kg/m}^3)(9.807 \text{ m/s}^2)(4 \text{ m})}{4(0.364)(0.4)(1 \text{ kg m/ N s}^2)} \left( 1 - \exp\left(\frac{-4(20 \text{ m})(0.364)(0.4)}{4 \text{ m}}\right) \right) \\ &= 35,668 \text{ N/m}^2 \text{ (or 5.2 psi)} \end{aligned}$$

To estimate the normal stress on the wall we apply Janssen's assumption

$$\begin{aligned} P_w &= K P_v \\ &= 0.4 (35,668 \text{ N/m}^2) \\ &= 14,267 \text{ N/m}^2 \text{ (2.1 psi)} \end{aligned}$$

(b) If the silo was filled with water instead of granular solids, the pressure at depth  $H$  is given by

$$\begin{aligned} P &= \frac{\rho g H}{g_c} \\ &= \frac{1000 \text{ kg / m}^3 (9.807 \text{ m / s}^2)(20 \text{ m})}{1 \text{ kg m / N s}^2} \\ &= 196,140 \text{ N / m}^2 \text{ (28.4 psi)} \end{aligned}$$

The result in (b) is a factor of about 13 times greater than the normal wall stress calculated in (a). This is due to the wall friction exerting a vertical upward force on the granular solids.

### 10.3.4 HOPPER ANGLE AND OUTLET SIZE FOR MASS FLOW HOPPERS

To size and design a hopper we determine the design necessary for mass flow operation based upon the material properties. The properties that are used in the design of a mass flow hopper are the effective angle of internal friction, the material flow function, and the angle of wall friction between the powder material and the wall material.

In a mass flow hopper during discharge the stress distribution is such that a stable arch or funnel flow do not occur and therefore the flow will not stop. This analysis can be used in the design of a new hopper or to check the suitability of an existing hopper for use with a particular material.

#### 10.3.4.1 The Material Flow Function

Whether a hopper operates in mass flow or funnel flow depends on the flow properties of the powder material and how it interacts with the hopper walls. One way of analyzing stresses in a solid is through Mohr Circles. Mohr circles relate shear stress to the normal stress.

Given normal and shear stresses on a solid block (Figure 10-10), it is possible to find an angle ( $\theta$ ) of a surface within the block such that the normal stress on the new surface is a maximum (or minimum) and the shear forces are zero.

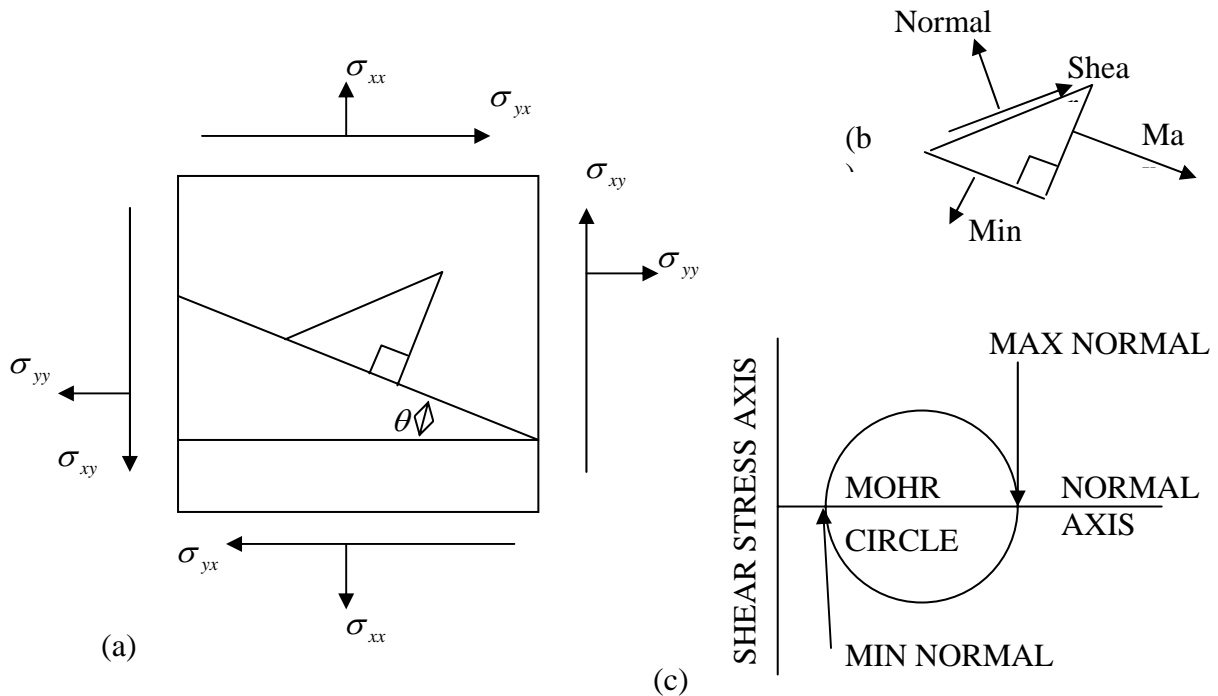


Figure 10-10. Stresses on a block. (a) Angle  $\theta$  is a surface with maximum/minimum normal force with zero shear. (b) Triangle shows maximum and minimum normal forces with no shear. (c) Mohr Circle.

Similarly, we can find an angle at which the shear stress is a maximum or minimum. Usually this occurs  $90^\circ$  from the maximum normal stress. The maximum and minimums are plotted on the stress plot (Figure 10-10 (c)).

For powder flow in a hopper, we want to know the shear stress needed to initiate flow (overcome the coefficient of static friction). A material's flowability depends upon the shear strength and how the shear strength changes with compacting stresses.

In experiments on a shear tester you must pre-stress the sample by applying a maximum load (critical point on the Jeniky Yield Locus (JYL) curve) and then reducing the applied stress during the experiments (Figure 10-11). Several different maximum loads are applied to generate at least three different JYL curves.

- If the material is cohesive, the JYL is not a straight line and does not pass through the origin. When extrapolated down to the zero shear stress the JYL crosses perpendicular to the Normal Stress axis.
- The JYL represents a surface that divides between operating conditions. Above the JYL the shear stress is sufficient to cause powder movement. Below the JYL the normal stress is too large for the powder to flow at the give shear stress.

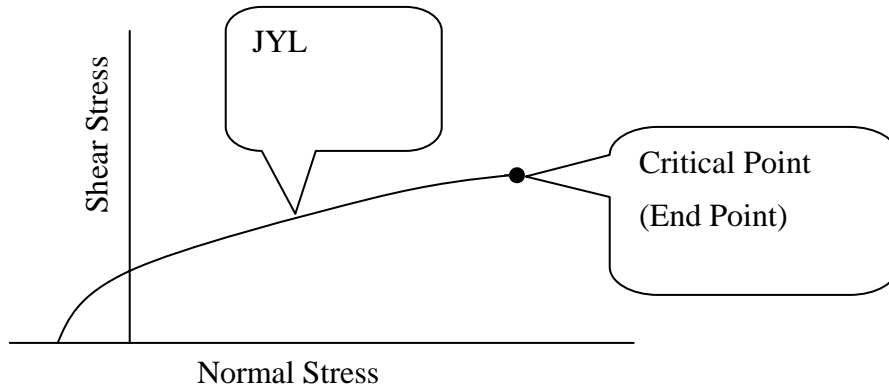


Figure 10-11. Jeniky Yield Locus (JYL) curve plotted from experimental data of Shear Stress versus Normal Stress for a given starting Critical Point.

Several Mohr Circles may be drawn that are tangent to the JYL. We are interested in two in particular.

1. The Mohr Circle passing through the origin and tangent to the JYL represents the stress needed to initiate flow in an arch (ie, to cause the arch to collapse) (Figure 10-12). The diameter of this Mohr Circle is the Unconfined Yield Stress (UYS),  $f_c$ .

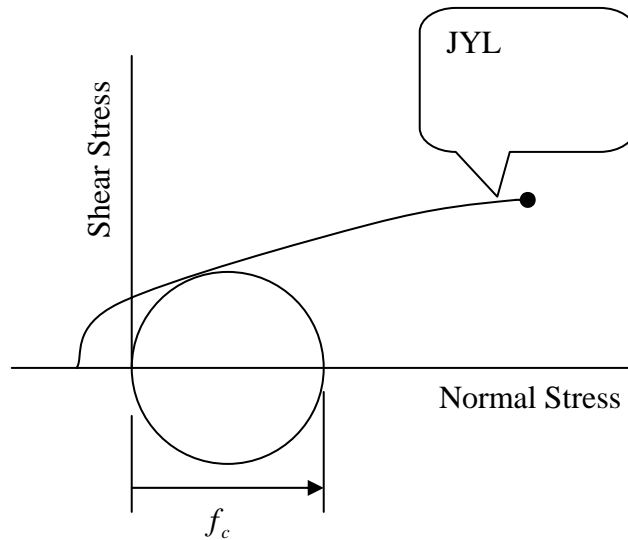


Figure 10-12. Mohr Circle passing through origin and tangent to the JYL. This is used to determine the value of  $f_c$ , the Unconfined Yield Stress (UYS).

2. The Mohr Circle passing through the critical point (end point) represents the state of the material at the compacting stress (Figure 10-13).

This represents the conditions for failure without volume change.

We assume it represents the stress conditions of the powder as it flows downward towards the outlet.

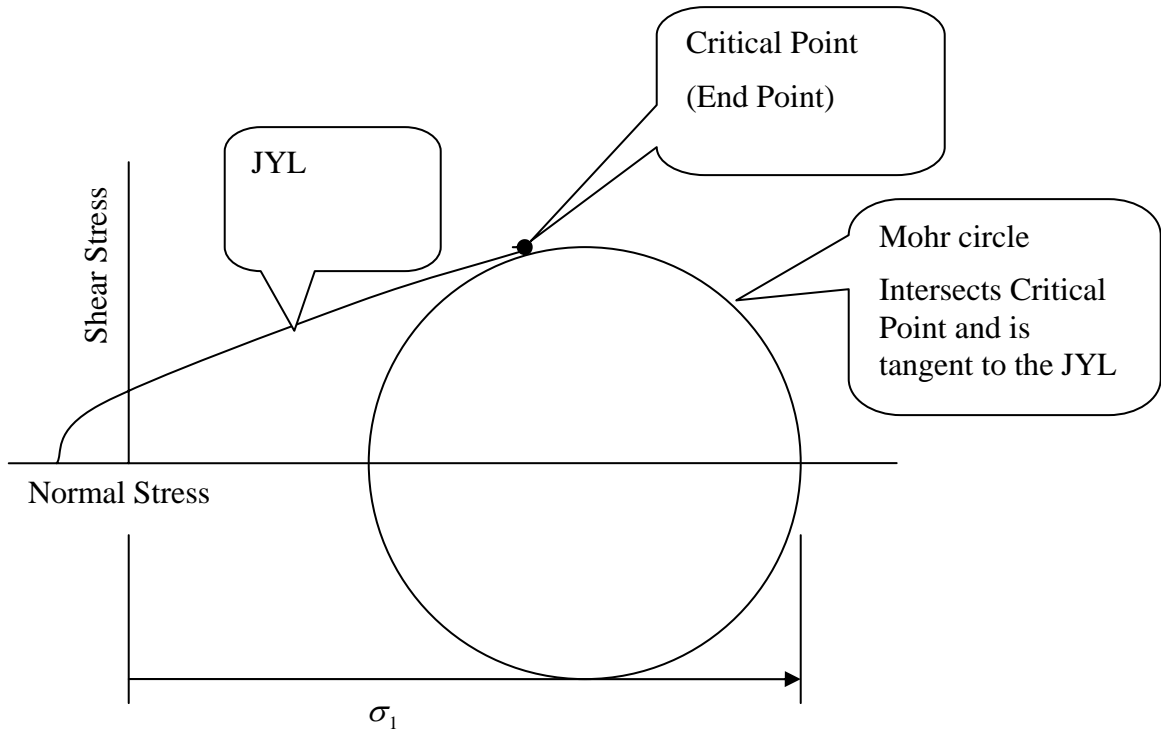


Figure 10-13. Mohr Circle passing through the critical point and tangent to the JYL. This is used to determine the value of  $\sigma_1$ .

Each JYL gives an  $f_c$  and  $\sigma_1$ . The  $f_c$  versus  $\sigma_1$  data are plotted to obtain the Material Flow Function (MFF) (Figure 10-14). The MFF curve represents the stress needed to make an arch collapse as a function of the compacting stress under which it was formed. Stresses below the MFF and the arch is stable. For points above the MFF the material is flowing and the frictional analysis in deriving the MFF does not apply.

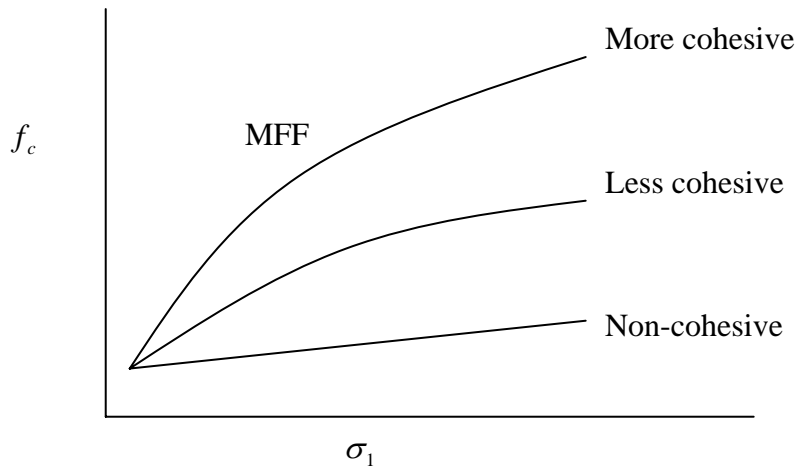


Figure 10-14. The Material Flow Function. More cohesive materials have larger  $f_c$  values. Non-cohesive materials have small  $f_c$  values.

### 10.3.4.2 The Effective Angle of Internal Friction

The effective angle of internal friction,  $\delta$ , is determined from the JYL plot.  $\delta$  is the angle of the slope of the line through the origin that is tangent to the Mohr Circles at the critical point, as shown in Figure 10-15.

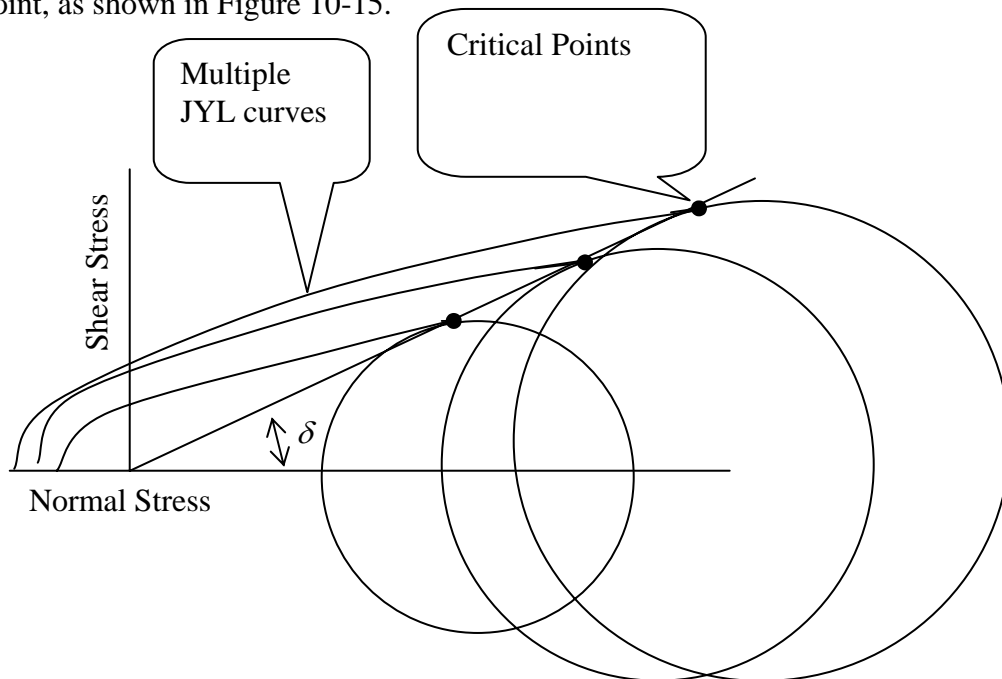


Figure 10-15. The angle  $\delta$  is the angle of the tangent line to the Mohr Circles at the critical points that passes through the origin.

### 10.3.4.3 The Angle of Wall Friction

The last property needed is the wall friction,  $\delta_w$ , between the powder and the wall of the hopper. This property is determined from experiments run with the shear tester as shown in Figure 10-5(a) where the measured shear force is plotted versus to the normal load (Figure 10-16). Often the data are linear. If they are nonlinear then the smallest angle is used.

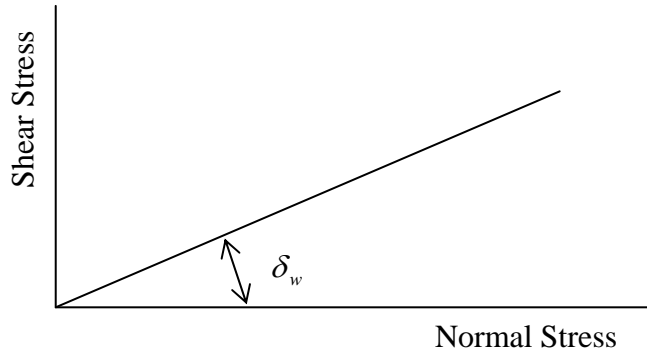


Figure 10-16. Plot to determine the wall angle,  $\delta_w$ .

### 10.3.4.4 Determining the Minimum Hopper Outlet Size

The forces acting on the powdered material stored in a hopper tend to (1) compact the powder (*i.e.*, reduce its bulk density), and (2) the shear stresses in the material tend to make it flow. Jenike (A.W. Jenike, Storage and Flow of Solids, Bulletin No. 123, Utah Engineering Experiment Station, University of Utah, Salt Lake City, Utah, 1964) showed that for an element at any position inside of a mass flow hopper, the ratio of the compacting stress to the shear stress has a constant value that he called the flow factor:

$$\text{flow factor, } ff = \frac{\text{compacting stress}}{\text{applied shear stress}} = \frac{\sigma_1}{AS} \quad (10-11)$$

Jenike published charts from which  $ff$  is determined. Charts for symmetrical slot outlet hoppers and for conical hoppers are shown in Figures 10-17 and 10-18.

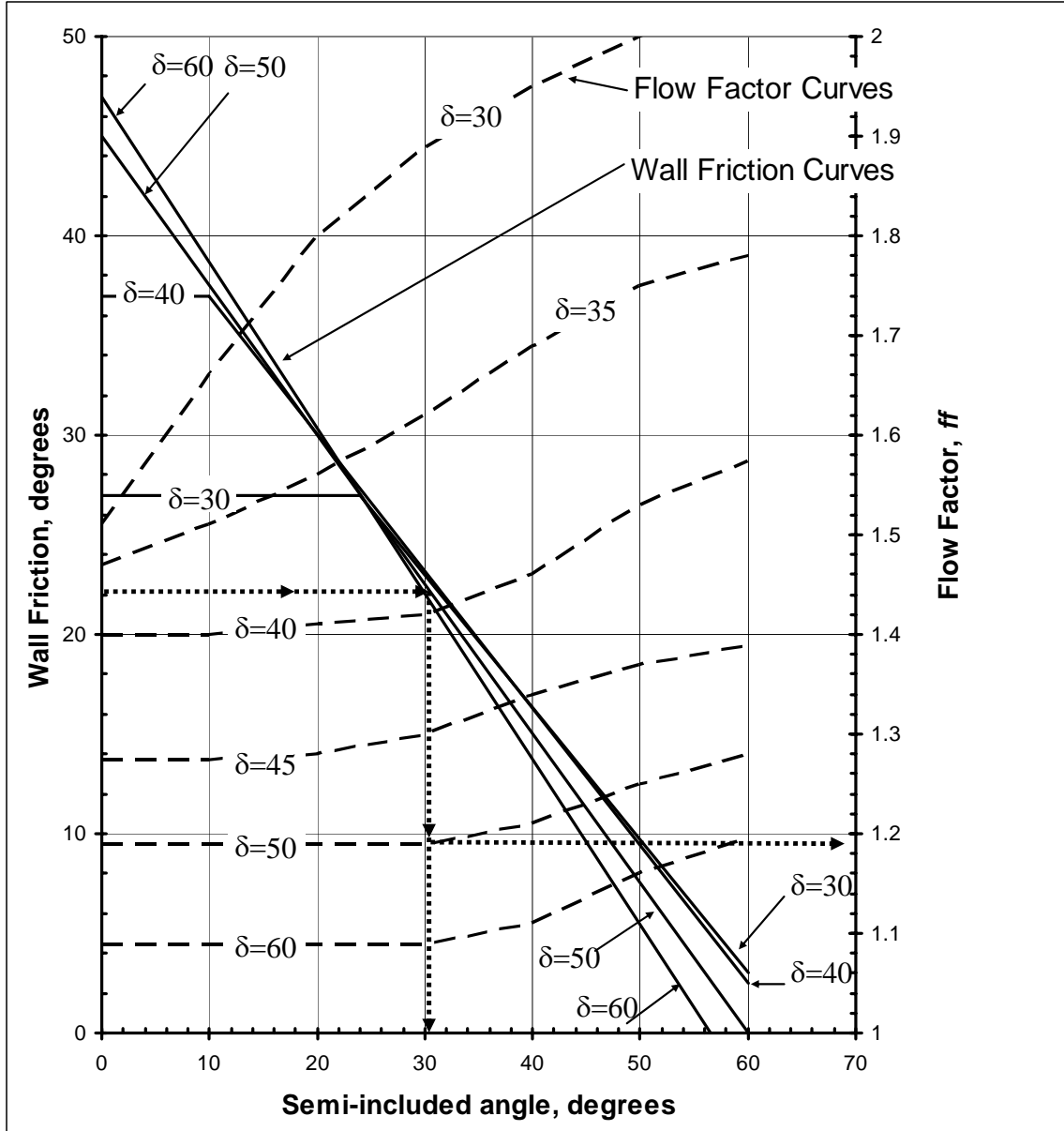


Figure 10-17. Design chart for symmetrical slot outlet hoppers. For example (dashed arrows),  $\delta_w = 22^\circ$  and  $\delta = 50^\circ$  gives  $\theta = 30.5^\circ$  and  $ff = 1.19$ .

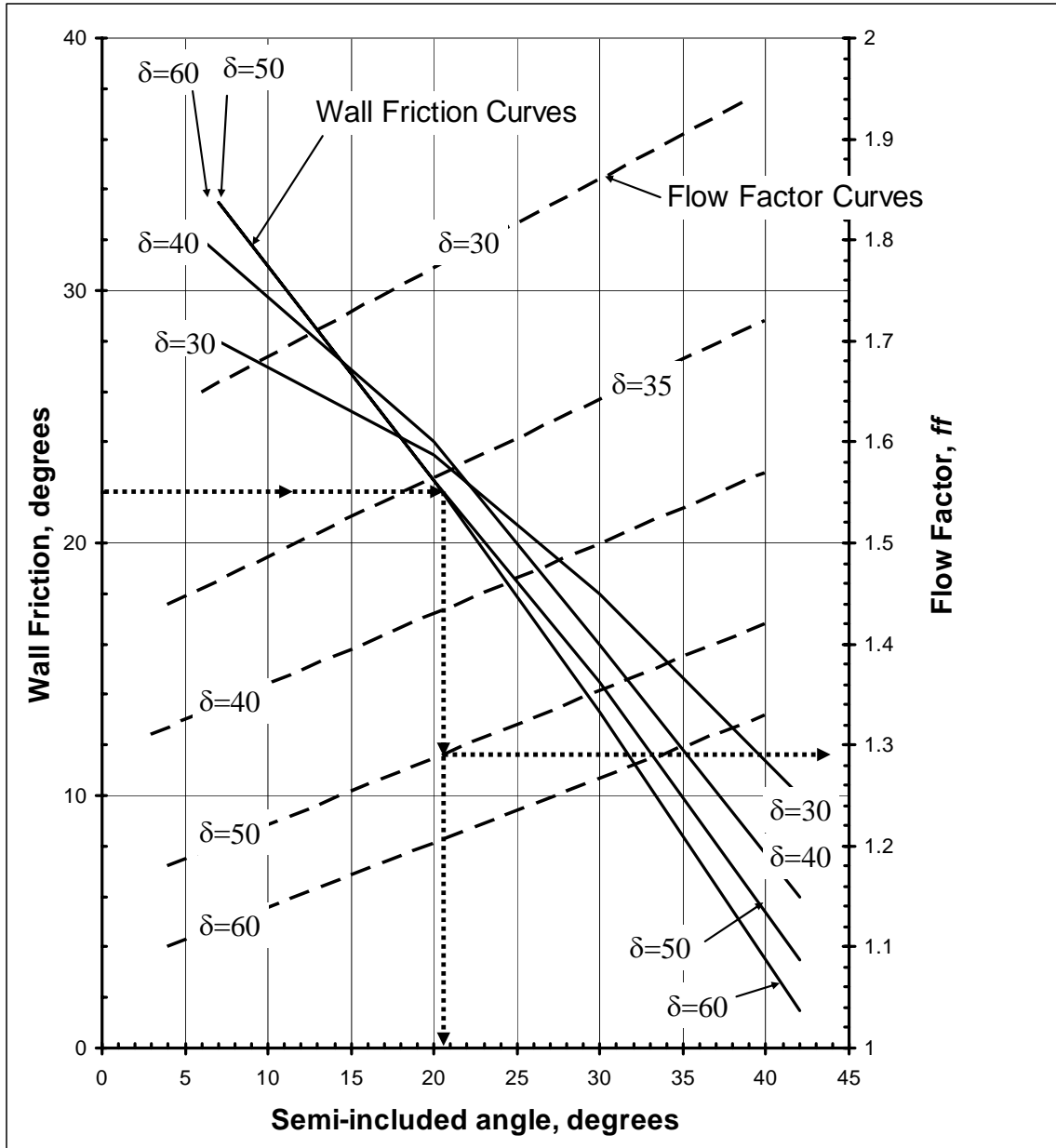


Figure 10-18. Design chart for conical outlet hoppers. For example,  $\delta_w = 22^\circ$  and  $\delta = 50^\circ$  gives  $\theta = 20.5^\circ$  and  $ff = 1.29$ .

The intersection of the MFF curve in Figure 10-14 with the line through the origin having a slope of  $1/ff$  is the Critical Applied Stress (CAS) (Figure 10-19). Recall that the condition of flow (no arching) occurs for points on or above the MFF curve. Therefore the hopper should operate where the  $1/ff$  curve is above the MFF curve, ie, above or to the right of the CAS.

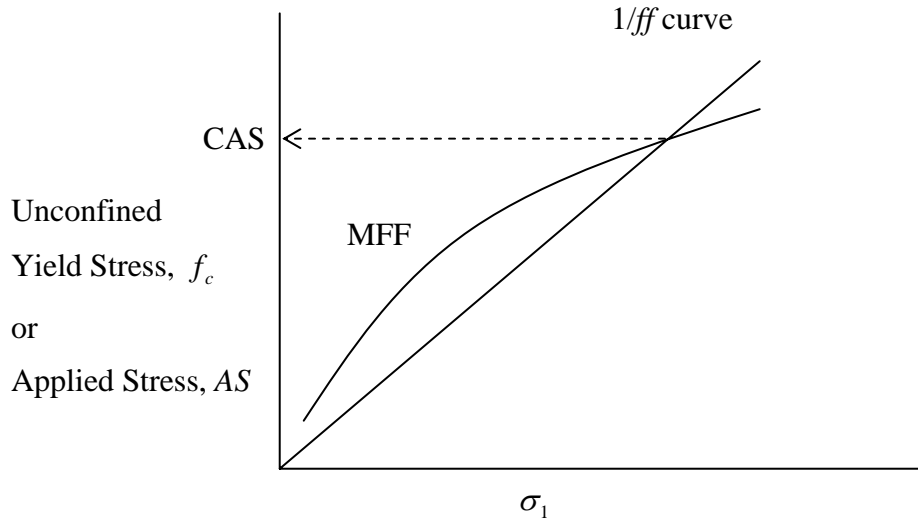


Figure 10-19. Intersection of the  $1/ff$  and MFF curves defines the Critical Applied Stress (CAS).

The stress in the outlet of the hopper may drop below the CAS if the opening is too small. Hence, the outlet opening size must ensure that the applied stress exceeds the CAS. Correlations relating the outlet size to the CAS are provided.

For conical hoppers, Figure 10-20, the opening diameter,  $D$ , is given by

$$D = H(\theta) \frac{CAS}{\rho^o g / g_c} \quad (10-12)$$

$$H(\theta) = 2 + \frac{\theta}{60} \quad (10-13)$$

Where  $\theta$  is in degrees, from the charts in Figures 10-17 or 10-18. Typical values for  $H$  are about 2.4.

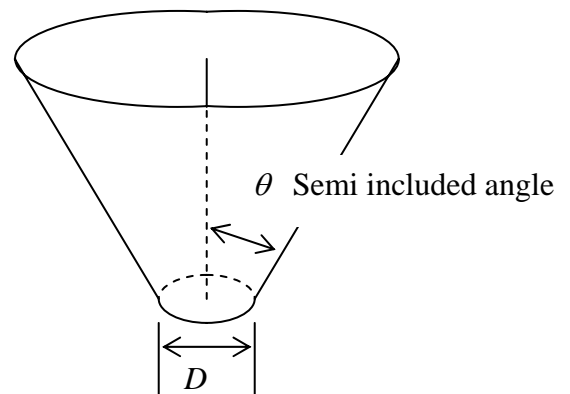


Figure 10-20. Conical Hopper with outlet size  $D$  and semi included angle  $\theta$ .

For symmetrical slot outlet hoppers the opening size is determined from

$$W = H(\theta) \frac{CAS}{\rho^o g / g_c} \quad (10-14)$$

$$H(\theta) = 1 + \frac{\theta}{180} \quad (10-15)$$

$$L > 3W \quad (10-16)$$

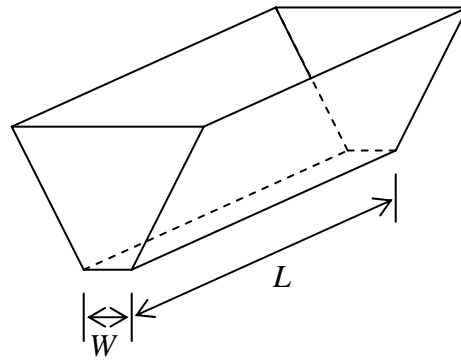


Figure 10-21. Symmetrical slot outlet hopper of opening size  $W \times L$ .

These are the minimum dimensions for the outlets to ensure mass flow. In the next section some correlations are given for estimating the flow throughput of the solids through the opening. Larger openings may be used for greater throughput and still maintain mass flow. In practical design the angle  $\theta$  is reduced by  $3^\circ$  as a margin of safety.

### EXAMPLE 10-2. EXAMPLE HOPPER DESIGN

The Shear Stress – Yield Stress JYL plots for a certain material yield the data in Table 10-2. Determine the wall slope and opening size to ensure mass flow in a conical hopper for this material. Assume the bulk density is  $1300 \text{ kg/m}^3$ .

Table 10-2. Experimental Shear Stress data on example powder.

<b>Shear Stress Internal Friction JYL Curve number (Figures 10-12 and 10-13)</b>	$\sigma_1$ (kPa)	$f_c$ (kPa)
1	2.4	0.97
2	2.0	0.91
3	1.6	0.85
4	1.3	0.78
<b>Wall Friction Measurements (Figure 10-16)</b>	Normal Force (kPa)	Shear Force (kPa)
1	2.0	0.689
2	3.0	1.03
<b>Effective Angle of Internal Friction, <math>\delta</math> (Figure 10-15)</b>	Rise, $\Delta y$ (kPa)	Run, $\Delta x$ (kPa)
Data taken from tangent line to Mohr Circle at critical point	1.0	1.73

*SOLUTION:*

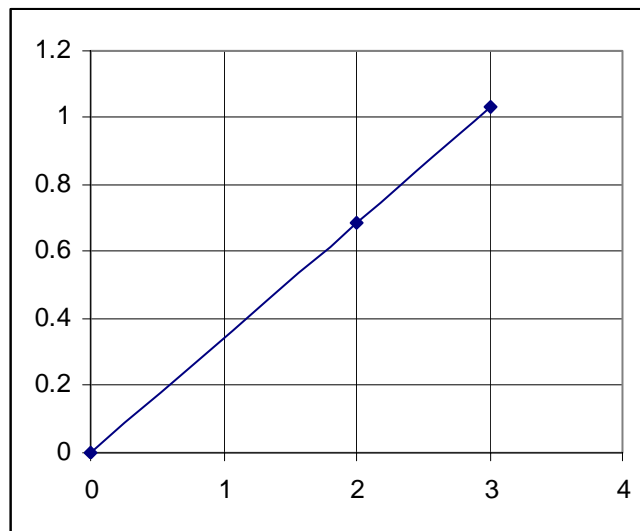
To get the effective angle of internal friction, the tangent of the angle is equal to rise/run.

$$\text{Tan}(\delta) = \frac{\Delta y}{\Delta x} = \frac{1.0}{1.73} = 0.76923$$

or, the angle is

$$\delta = \arctan(0.578) = 30^\circ$$

To get the wall friction angle the given data points are plotted as in Figure 10-16.



From which we see the data are linear. The angle is easily found from the rise/run as before

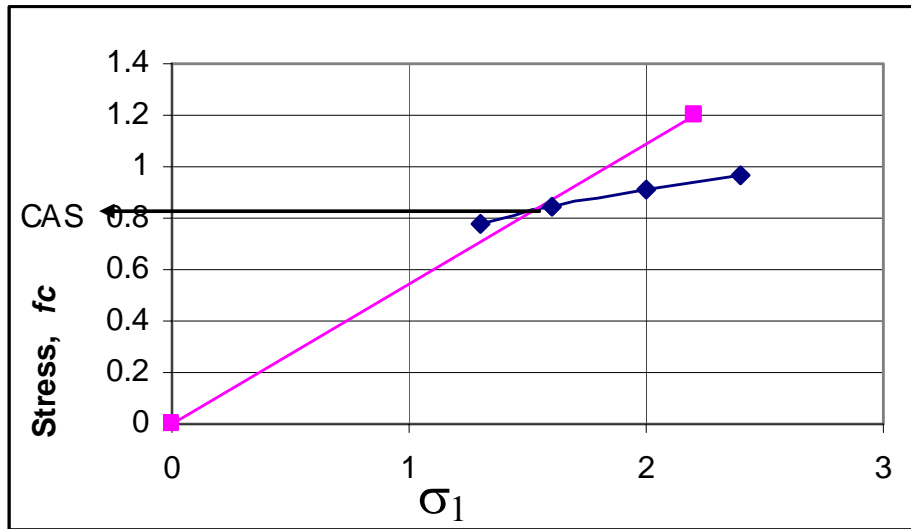
$$\text{Tan}(\delta_w) = \frac{\Delta y}{\Delta x} = \frac{1.03}{3.0} = 0.3433$$

or, the angle is

$$\delta_w = \arctan(0.3433) = 19^\circ$$

From Figure 10-18 we get the semi included angle  $\theta = 28^\circ$  and the flow factor  $ff = 1.84$ .

The  $f_c$  vs  $\sigma_1$  data are plotted to obtain the Material Flow Function (MFF), and the  $ff$  value is used to plot the  $1/ff$  curve as in Figure 10-19, to obtain the CAS value



Hence, the CAS = 0.83 kPa.

From Eq. 10-13

$$H = 2.47$$

From Eq.10-12

$$D = 2.47 \cdot \frac{(0.83 \text{ kPa})(1000 \text{ Pa / kPa})(1 \text{ N / m}^2 / \text{ Pa}) \frac{1 \text{ kg m}}{\text{N s}^2}}{1300 \text{ kg / m}^3 (9.807 \text{ m / s}^2)}$$

$$= 0.161 \text{ m}$$

Hence, for a mass flow conical hopper the minimum diameter of the opening is 0.161 m. As a margin of safety, the semi included angle is reduced by 3 degrees and the hopper design angle is 25 degrees.

### 10.4 Rate of Discharge from Hoppers

There are a number of methods for calculating discharge rates from silos or hoppers. A few of the equations are provided here.

#### 10.4.1 COARSE PARTICLES

For coarse particles (particles > 500 microns in diameter) there are two equations commonly used, one for mass flow and one for funnel flow

##### MASS FLOW – JOHANSON EQUATION

The Johanson equation, derived from fundamental principles (Trans. Min. Engrs. AIME, **232**, 69-80, (1965); Trans. ASME, 224-230 (1966) is

$$\dot{m} = \rho^o A \sqrt{\frac{Bg}{2(1+m)\tan(\theta)}} \quad (10-17)$$

- where
- $\theta$  = semi included angle of the hopper
  - $\dot{m}$  = discharge rate (kg/sec)
  - $\rho^o$  = bulk density (kg/m<sup>3</sup>)
  - $g$  = gravity acceleration (9.807 m/s<sup>2</sup>)

Depending on whether a conical or symmetric slot opening hopper the remaining parameters in the equation are given in Table 10-3.

Table 10-3. Parameters in the Johanson Equation, Eq.(10-18)

Parameter	Conical hopper	Symmetric slot hopper
B	$D$ , diameter of outlet	$W$
A	$\frac{\pi}{4} D^2$	$WL$
m	1	0

##### FUNNEL FLOW – BEVERLOO EQUATION

A theoretical expression for funnel flow discharge is not available. Beverloo (W.A. Beverloo, H.A. Leniger, J. van de Velde, The Flow of Granular Solids Through Orifices, Chem Eng Sci, **115**, 260-269, 1961) tested a variety of seeds and derived an empirical equation. The Beverloo Equation is

$$\dot{m} = 0.58 \rho^o g^{0.5} (D - kd_p)^{2.5} \quad (10-18)$$

- where
- $d_p$  = particle diameter (m)

$k = \text{constant}$ , typically  $1.3 < k < 2.9$  with  $k = 1.4$  if not discharge rate data are available. The term  $kd_p$  accounts for the wall effect where the particles do not fully flow at the perimeter of the outlet.

$D = \text{outlet diameter (m)}$ . For non-circular outlets the hydraulic diameter is used

$$D = \frac{4(\text{cross sectional area})}{(\text{outlet perimeter})}$$

The remaining parameters are defined as in Eq.(10-17).

### 10.4.2 FINE PARTICLES

Fine particles ( $d_p < 500$  microns) tend to flow slower by a factor of 100 to 1000 than that predicted by the Johanson equation. The reason for this is the effect of air drag on the motion of the particles is much greater for fine particles.

Particle beds need to dilate (increase distance between particles) before the powder can flow. This means air must penetrate into the bed through the bottom surface of the hopper as the powder moves through the constriction formed by the conical walls. For fine particles the pore diameters in the powder bed are small and there is a significant amount of air drag that resists the powder motion.

Carleton gives an expression for predicting the velocity of the solids as (Powder Tech., 6, 91-96, 1972)

$$\frac{4V_o^2 \sin \theta}{B} + 15 \frac{\rho^{1/3} \mu^{2/3} V_o^{4/3}}{\rho_p d_p^{5/3}} = g \quad (10-19)$$

$$\dot{m} = \rho^o A V_o$$

where  $V_o = \text{average velocity of solids discharging (m/s)}$

$A, B = \text{given in Table 10-3}$

$\rho, \mu = \text{air density and viscosity}$

$\rho_p = \text{particle density}$

$\rho^o = \text{bulk density of the powder bed}$

The remaining parameters are defined with Equations (10-17) and (10-18).